Journal of Peptide Science
J. Peptide Sci. **7**: 197–207 (2001)
DOI: 10.1002/psc.320

Peptide T Revisited: Conformational Mimicry of Epitopes of Anti-HIV Proteins

DELIA PICONE[a,*], ANGELA RIVIECCIO[a], ORLANDO CRESCENZI[b], GIUSEPPE CALIENDO[c], VINCENZO SANTAGADA[c], ELISA PERISSUTTI[c], SUSANNA SPISANI[d], SERENA TRANIELLO[d] and PIERO ANDREA TEMUSSI[a]

[a] Dipartimento di Chimica, Università degli Studi di Napoli 'Federico II', Complesso Universitario di Monte S. Angelo, Napoli, Italy
[b] Dipartimento di Chimica Organica e Biochimica, Università degli Studi di Napoli 'Federico II', Complesso Universitario di Monte S. Angelo, Napoli, Italy
[c] Dipartimento di Chimica Farmaceutica e Tossicologica, Università degli Studi di Napoli 'Federico II', Napoli, Italy
[d] Dipartimento di Biochimica e Biologia Molecolare, Università di Ferrara, Ferrara, Italy

Received 15 November 2000
Accepted 8 January 2001

Abstract: Peptide T (ASTTTNYT), a fragment corresponding to residues 185–192 of gp120, the coat protein of HIV, is endowed with several biological properties *in vitro*, notably inhibition of the binding of both isolated gp120 and HIV-1 to the CD4 receptor, and chemotactic activity. Based on previous nuclear magnetic resonance (NMR) studies performed in our laboratory, which were consistent with a regular conformation of the *C*-terminal pentapeptide, and SAR studies showing that the *C*-terminal pentapeptide retains most of the biological properties, we designed eight hexapeptides containing in the central part either the TNYT or the TTNY sequence, and charged residues (D/E/R) at the two ends. Conformational analysis based on NMR and torsion angle dynamics showed that all peptides assume folded conformations, albeit with different geometries and stabilities. In particular, peptides carrying an acidic residue at the *N*-terminus and a basic residue at the *C*-terminus are characterized by stable helical structures and retain full chemotactic activity. The solution conformation of peptide ETNYTR displays strong structural similarity to the region 19–26 of both bovine pancreatic and bovine seminal ribonuclease, which are endowed with anti-HIV activity. Moreover, the frequent occurrence, in many viral proteins, of TNYT and TTNY, the two core sequences employed in the design of the hexapeptides studied in the present work, hints that the sequence of the *C*-terminal pentapeptide TTNYT is probably representative of a widespread viral recognition motif.

Keywords: chemotactic activity; conformation; HIV; NMR; peptide T

INTRODUCTION

It has been proposed that the interaction between HIV-1 and its receptors in the host cell could involve the region 185–192 of the gp120 coat protein [1]. The synthetic fragment corresponding to this sequence (ASTTTNYT), dubbed peptide T after its high Thr content, was shown to inhibit the binding of both isolated gp120 and HIV-1 with the CD4 receptor. These original observations have not been

Abbreviations: Fmoc, 9-fluorenylmethoxycarbonyl; DIPCDI, 1,3-diisopropylcarbodiimide; HOBt, 1-hydroxybenzotriazole; TFA, trifluoroacetic acid; Et_3SiH, triethylsilane; PITC, phenyl isothiocyanate.

* Correspondence to: Dipartimento di Chimica, Università degli Studi di Napoli 'Federico II', via Cintia, Complesso Universitario di Monte S. Angelo, 80126 Napoli, Italy; e-mail: picone@chemistry.unina.it

followed by successful clinical applications. On the contrary, since then many controversial data have been reported on the actual *in vitro* activity of peptide T and on its possible therapeutical application. As a consequence, interest in the SAR of peptide T and analogues as possible anti-HIV drugs has declined.

Later on, it has been shown that the invasion of healthy cells by HIV-1 requires the sequential interaction of the gp120 envelope protein with at least two cell surface molecules: the CD4 primary receptor and a co-receptor, belonging to the chemokine receptor family of seven-helices membrane spanning receptors [2]. The majority of HIV-1 specimens directly isolated from patients need CCR-5 as co-receptor, whereas so-called 'laboratory adapted' isolates of HIV-1 use a distinct coreceptor molecule termed CXCR-4 instead of, or in addition to, CCR-5 [3]. The recent determination of crystal-structure of gp120 in a ternary complex with CD4 receptor and a neutralizing human antibody [4], while rekindling the interest in gp120, does not clarify the controversial role of peptide T in the interaction. The neutralizing human antibody, called 17b, partially mimics the HIV-1 co-receptor (either CCR-5 or CXCR-4), but the recombinant gp120 utilized in this study was a 'core fragment' depleted of some variable regions including the region encompassing peptide T (the variable region V2). However, the likely structure of the loop V1/V2, modelled and adapted to the remaining crystal-structure, is located above the gp120 core, close to the contact region with the antibody fragment [4]. Moreover, the authors of this study suggest that CD4 binding triggers a conformational transition of gp120, which moves the V1/V2 loop still closer to the co-receptor. It is, therefore, conceivable that the region V2, which contains the sequence of peptide T, may be involved in an interaction with the chemokine receptor, instead of or in addition to the CD4 receptor.

It is interesting to note that peptide T is endowed, among other biological activities [5], with a potent chemotactic activity on human monocytes, which is correlated with the inhibition of CD4 binding [6,7]. The involvement of peptide T in an interaction with a protein belonging to the chemokine receptor family, implying a possible interpretation for its chemotactic activity, prompted us to undertake new SAR studies on this peptide and its analogues.

In the present study, we have designed a series of hexapeptides containing in the central part the essential core of peptide T (either the TNYT or the TTNY sequence) flanked by charged residues at the two ends. We have synthesized eight such peptides, characterized by the presence at the terminals of arginine (R) as a basic residue and aspartate (D) or glutamate (E) as an acidic residue, i.e. by the pairs D/R, E/R R/D and R/E. All peptides were examined by means of a classical chemotactic test and studied in solution by a combination of nuclear magnetic resonance (NMR) spectroscopy and torsion angle dynamics.

MATERIAL AND METHODS

General Procedure for Solid-phase Synthesis of Peptides I–VIII

All peptides (**I**: D-TNYT-R; **II**: E-TNYT-R; **III**: D-TTNY-R; **IV**: E-TTNY-R; **V**: R-TNYT-D; **VI**: R-TNYT-E; **VII**: R-TTNY-D; **VIII**: R-TTNY-E) were prepared by the solid-phase method with a continuous-flow instrument with on-line ultraviolet (UV) monitoring (Milligen/Biosearch 9050). The stepwise syntheses were carried out by 9-fluorenylmethoxycarbonyl (Fmoc) chemistry. No special efforts were made to optimize the repetitive steps. For each peptide, 0.5 g (0.35 mequiv) of Wang resin (Novabiochem, Laufelfingen, Switzerland) was used. The functionalized resin was swelled in *N*,*N*-dimethylformamide (DMF) for 1 h and packed in the reaction column. *tert*-Butyl was used as a side-chain protecting group for Thr, Asp, Tyr and Glu while Pmc and Trt were used for Arg and Asn, respectively. N^{α}-Fmoc amino acids were used in a four-fold excess using 1,3-diisopropylcarbodiimide (DIPCDI) in the presence of 1-hydroxybenzotriazole (HOBt) for 1 h. The Fmoc group was removed with a flow of 20% piperidine in DMF for 25 min. After completion of the synthesis each protected peptide was cleaved from the resin, and the amino acid side chains were simultaneously deprotected by treatment with 7 mL of trifluoroacetic acid (TFA)/H_2O/triethylsilane (Et_3SiH) (88:5:7) mixture for 1 h at room temperature (rt). The resin was removed by filtration and washed with TFA (2 × 1 mL), the filtrate and washings were combined and evaporated at 25°C, and the oily residue was triturated with diethyl ether (10 mL). The resulting solid peptide was collected by centrifugation and purified by preparative reverse-phase high performance liquid chromatography (RP-HPLC) (purification yield, 75–85%). Structural verification was achieved by amino acid analysis, mass spectrometry, and NMR spectroscopy (Table 1).

Table 1 Analytical Data on Peptide T Analogues

Peptide	Amino acid composition					FAB MS m/z	
						Calculated	Found
I	**Asp**	**Thr**	**Tyr**	**Arg**		768.77	769.10
	2.00	1.97	0.98	0.97			
II	**Glu**	**Thr**	**Asp**	**Tyr**	**Arg**	782.80	783.40
	0.98	1.92	0.97	0.96	1.01		
III	**Asp**	**Thr**	**Tyr**	**Arg**		768.77	769.10
	2.01	1.95	0.97	0.96			
IV	**Glu**	**Thr**	**Asp**	**Tyr**	**Arg**	782.80	783.40
	1.01	1.95	1.01	0.89	0.92		
V	**Arg**	**Thr**	**Asp**	**Tyr**		768.77	769.10
	0.93	1.95	2.01	0.88			
VI	**Arg**	**Thr**	**Asp**	**Tyr**	**Glu**	782.80	783.40
	0.98	1.90	1.02	0.88	0.98		
VII	**Arg**	**Thr**	**Asp**	**Tyr**		768.77	769.10
	1.02	1.93	2.02	0.93			
VIII	**Arg**	**Thr**	**Asp**	**Tyr**	**Glu**	782.80	783.40
	1.02	1.97	1.01	0.96	1.02		

Homogeneity and retention times of the purified products were assessed by analytical RP-HPLC with a Vydac C18-column (10 μm, 3.9 × 250 mm, spherical) connected to a Rheodyne Model 7725 injector, an Altex 420 HPLC system using two Altex 100 A pumps, a Waters 486 tunable absorbance detector set to 220 nm, and a SE-120 strip chart recorder. Analytical determinations were carried out with the following gradient system: A, 0.1% TFA in CH_3CN; B, 0.1% TFA in H_2O; linear gradient from 0% A–100% B to 30% A–70% B over 30 min, flow rate 1 mL/min. The final HPLC purity of the peptides was always greater than 99%.

Preparative RP-HPLC was routinely performed on a Waters Delta-Prep 4000 system equipped with a Waters 486 multiwavelength detector, using a Vydac C-18 (15-20 μm, 20 × 250 mm) column. The gradient used was the same as for the analytical determinations. The flow rate was 30 mL/min.

Thin-layer chromatography was performed on precoated silica gel plates Kieselgel 60 F254 (Merck, Darmstadt, Germany) with the following solvent systems: A, $CHCl_3$-MeOH (methanol) (10:1); B, $CHCl_3$-MeOH (20:1); C, $CHCl_3$-MeOH-AcOH (acetic acid) (8:1:1). The products on thin-layer chromatography plates were detected by UV light and either chlorination followed by a solution of 1% starch-15 KI or ninhydrin. Extraction solvents were dried over magnesium sulfate. Solvents used for reactions were dried over 3 Å molecular sieves. DMF was distilled immediately before use over CaH_2. All solvents were filtered and degassed prior to use. Reagent grade materials were purchased from Novabiochem and from Sigma–Aldrich (Milano, Italy), and were used without further purification. Amino acid analyses were carried out using phenyl isothiocyanate (PITC) methodology (Pico-Tag, Waters–Millipore, Waltham, MA). Lyophilized samples of peptides (50–100 pmol) were placed in heat-treated borosilicate tubes (50 × 4 mm), sealed, and hydrolysed using 200 μL of 6 N HCl containing 1% phenol in the Pico-Tag work station for 1 h at 150°C. A Hypersil ODS column (250 × 4.6 mm, 5 μm particle size) was employed to separate the PITC-amino acid derivatives.

Molecular weights of peptides were determined by fast-atom bombardment mass spectrometry (FAB/MS) on a ZAB 2 SE-Fisons.

Monocyte Chemotaxis

Mononuclear cells were isolated from heparinized blood of normal human volunteers by sedimentation over Ficoll-Paque (Pharmacia, Uppsala, Sweden), and chemotaxis assays were performed in a modified Boyden chamber, using a 48 multiwell chemotaxis chamber (Neuroprobe, Inc., Milano, Italy), by measuring the distance (μm) covered by the migration of the leading front [8], as previously described [9]. Each compound was dissolved in dimethylsulfoxide (DMSO) at a concentration of

10^{-2} M, diluted before use with Krebs–Ringer phosphate buffer containing 0.5 mg/mL bovine serum albumin (Sigma-Aldrich), and tested at a final concentration in the range 10^{-12}–10^{-5} M. To obtain an accurate comparison, the results for the individual compounds are expressed in terms of chemotactic index (C.I.), which is the ratio: (migration towards test attractant minus migration towards the buffer)/migration towards the buffer. Migration in presence of the buffer alone was 35 μm ± 3 S.E. ($n = 8$). In all experiments 10^{-8} M For-Met-Leu-Phe-OH was used as a peptide control; peak response migration was 67 μm ± 3 S.E. (C.I. 0.92 ± 0.03).

NMR

For use in NMR experiments, each peptide was dissolved in water, pH was adjusted to a value between 6 and 7 by small addition of 1 M NaOH, and aliquots corresponding to about 1 mg of peptide were lyophilized. Two aliquots were taken up in 500 μL of the required solvent to make up a NMR sample. Spectra were collected at 400 MHz on a Bruker DRX-400 instrument. One-dimensional NMR spectra were acquired in the temperature range 295–330 K, in the Fourier mode, with quadrature detection, and the water signal was suppressed by a low-power selective irradiation in the homogated mode. Assignments of ^{1}H resonances were achieved by a combination of standard two-dimensional experiments (DQF-COSY [10], TOCSY [11] and NOESY [12]). All experiments were run in the phase-sensitive mode using quadrature detection in ω_1 by time-proportional phase incrementation of initial pulse [13]. Data block sizes were 2048 addresses in t_2 and 350 equidistant t_1 values. Before Fourier transformation, the time domain data matrices were multiplied by shifted cosine functions in both dimensions. A mixing time of 70 ms was employed for the TOCSY experiment. NOESY experiments were run at 275–280 K with mixing times in the range 150–300 ms. Cross-peak volumes were quantitated from NOESY spectra with 200, 250 and 300 ms mixing times, using the NMRView software [14].

Structure Calculations

Peak lists were converted into the format used by DYANA 1.5 [15] and translated into upper distance bounds with the routine CALIBA: the necessary pseudoatom corrections were applied for non-stereospecifically assigned protons at prochiral centers and for the Thr methyl group. A total of 40 random initial structures were generated and subjected to restrained simulated annealing in torsion angle space, using the standard protocol of DYANA.

The 10 DYANA structures with the lowest target function values were refined by restrained minimization with the SANDER module of AMBER 5.0 [16]. The '1991' all-atom force field was used, with a distance-dependent dielectric constant $\varepsilon = r_{ij}$. A distance cutoff of 12 Å was used in the evaluation of non bonded interactions. Distance restraints were applied as a flat well with parabolic penalty within 0.5 Å outside the upper bound, and a linear function beyond 0.5 Å, using a force constant of 6.4 kcal/mol/Å^2. Computations were performed on SGI O2 computers.

RESULTS

Peptide Design

Peptide T, and shorter fragments thereof, have been the object of several conformational studies, based mainly on NMR and/or theoretical calculations [17–20]. In all cases it has been reported that, in spite of its small size, this peptide shows a high tendency to assume folded conformations, while retaining a considerable flexibility, as expected for all linear peptides. The first NMR study, performed in our laboratory [17], hinted that, in DMSO, the prevailing conformation is a quasi-cyclic conformer characterized by a β-turn centred on the *N-Y* sequence. However, the spectroscopic data did not rule out the possibility of a helical structure (either α or 3_{10}) involving residues 4–8 [21]. Previous SAR studies on peptide T had shown that the *C*-terminal pentapeptide retains most of the biological properties, notably chemotactic activity [22]. Based on these results, we have designed a series of hexapeptides containing either the TNYT or the TTNY sequence in the central part, flanked by residues carrying opposite charges at the two ends, that is, peptides of general formula [R/D, E]-TNYT-[D, E/R] and [R/D, E]-TTNY-[D, E/R]. The rationale of this choice is that the oppositely charged residues at the two ends might enhance the intrinsic tendency of peptide T towards pseudo-cyclization. A screening of the chemotactic activities of such peptides, in combination with conformational studies in solution, should provide useful clues on the bioactive conformation of peptide T and its role in the interaction with host cell receptors.

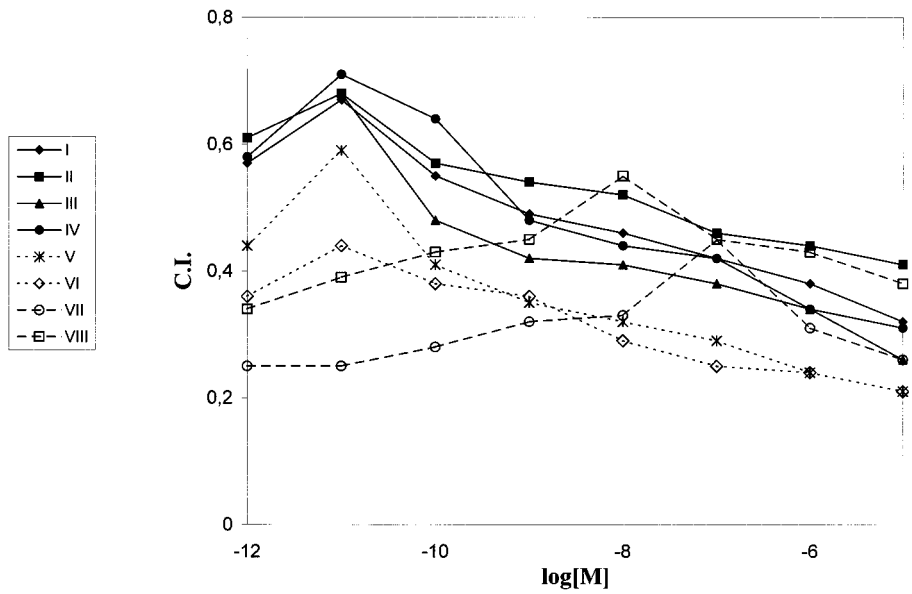

Figure 1 Migration of human monocytes in response to concentration gradients, ranging from 10^{-12} to 10^{-5} M. The experimental points of C.I. are the mean of five separate experiments. S.E.s are within 10% of the mean value.

Chemotactic Activity

The biological activity of the hexapeptides I–VIII was assessed by measuring their ability to stimulate monocyte directed migration (chemotaxis). Figure 1 reports, for all peptides, the migration of monocytes in response to concentration gradients ranging from 10^{-12} to 10^{-5} M. While all analogues retain a substantial chemotactic activity, the charges introduced at the two terminals modulate the activity to a large extent. Based on their activity, the peptides can be grouped in three families. Peptides I–IV, hosting an acidic residue at the *N*-terminus, display the highest chemotactic potencies and efficacies, with a maximum value of C.I. of about 0.70 at a peptide concentration of 10^{-11} M. Peptides V and VI have reduced potency, but an efficacy comparable to that of peptides I–IV (0.60 and 0.44 C.I., respectively, at 10^{-11} M). Peptides VII and VIII have both low potency and low efficacy. At first sight, the finding that the most active peptides carry an acidic residue at the *N*-terminus and a basic residue at the *C*-terminus seems to contradict the expectation that a pseudocyclization ought to favour the bioactive conformation. However, the complexity of the conformation-activity relationship precludes a simplistic analysis based solely on constitution and calls for a detailed conformational analysis.

NMR Conformational Analysis

As a general rule, linear hexapeptides are very flexible and rarely exist as single ordered conformers in solution. However, judicious choice of solution conditions, i.e. solvent medium and temperature, can still reveal conformational tendencies of the peptides in different environments. We performed an ^{1}H NMR analysis in water, neat organic solvents (CD_3CN, DMSO) and aqueous mixtures of organic solvents [DMSO/water, HFA(1,1,1,3,3,3-hexafluoroacetone)/water]. Preliminary results, based mainly on the spread of NH resonances and the number of NOEs, showed that all peptides are completely disordered in water and show progressively higher tendency towards ordered conformations in aqueous mixtures and neat organic solvents. It is worth emphasizing that spectra in HFA/water, a strong helix-inducing medium [23], are poorer than those in DMSO. This is somewhat surprising, since DMSO is known to solvate backbone NHs very strongly and, therefore, in general to favour extended conformations. However, in a few cases this solvent already proved to favour folded conformers, e.g. peptide T itself [17], tuftsin [24] and even larger peptides [25]. It is also worth noting that the improvement of the quality of the NMR spectra and the very presence of ordered conformers in DMSO solutions seem linked to the presence, in the peptides, of residues with hydroxyl groups in the side chain. This effect is akin

to what is routinely observed in NMR spectra of carbohydrates in DMSO solutions. It is tempting to attribute these effects to the efficient solvation by DMSO of the side chain-OH groups that would otherwise interfere with backbone hydrogen bonds. Another interesting aspect of DMSO is that a medium with a viscosity higher than water (η of DMSO is *ca.* 3.5 cp at rt) can reproduce at least one of the physicochemical features of membranes and cytoplasm [26]. We decided to perform our study in DMSO, the solvent that, on average, afforded best structuring conditions for all the peptides.

Table 2 Chemical Shifts (ppm) at 300 K and Temperature Coefficients (ppb/K) of Amide Protons of Peptides I, II, III, VII and VIII in DMSO-d_6

	I	**II**	**III**	**VII**	**VIII**
Res1		E	D	R	R
HN	n.d.	n.d.	n.d.	n.d.	n.d.
Hα	3.81	3.46	3.95	n.d.	3.50
Hβ1/β2	2.42, 2.54	1.70, 1.88	2.60	1.30	1.72
Hγ1/γ2	–	2.27	–	1.60	1.60
Hδ1/δ2	–	–	–	3.17	3.13
Res2	T	T	T	T	T
HN	n.d.	8.28	n.d.	n.d.	n.d.
Hα	4.16	4.22	4.27	n.d.	n.d.
Hβ	4.06	4.01	4.03	4.17	n.d.
Hγ	1.05	1.02	1.05	1.10	n.d.
$\Delta\delta/\Delta T$	n.d.	n.d.	−4.8	n.d.	n.d.
Res3	N	N	T	T	T
HN	8.27	8.20	7.96	7.79	7.92
Hα	4.45	4.50	4.25	4.32	4.32
Hβ1/β2	2.46	2.53, 2.41	n.d.	4.15	4.12
Hγ	–	–	1.13	1.08	1.10
Others	6.96, 7.58	6.98, 7.45	–	–	–
$\Delta\delta/\Delta T$	−2.6	−2.3	−4.8	−4.8	−4.2
Res4	Y	Y	N	N	N
HN	8.02	7.97	8.15	8.14	8.28
Hα	4.37	4.41	4.50	4.53	4.55
Hβ1/β2	2.76, 2.97	2.72, 2.98	2.52	2.45, 2.60	2.43, 2.58
Others	7.02, 6.64	6.63, 7.03	7.36, 7.01	7.38, 7.02	7.40, 6.96
$\Delta\delta/\Delta T$	−1.7	−2.4	−4.3	−5.2	−6.8
Res5	T	T	Y	Y	Y
HN	7.91	7.92	8.05	7.96	7.92
Hα	4.16	4.16	4.30	4.30	4.25
Hβ1/β2	4.00	4.00	2.76, 2.99	2.68, 2.97	2.74, 3.05
Hγ	1.02	1.01	–	–	–
Others	–	–	7.03, 7.60	6.98, 6.68	7.02, 6.70
$\Delta\delta/\Delta T$	−5.3	−7.0	−4.8	−4.2	−3.6
Res6	R	R	R	D	E
HN	7.58	7.56	7.58	7.65	7.48
Hα	3.92	3.89	3.94	4.12	3.97
Hβ1/β2	1.58, 1.70	1.59, 1.68	1.59, 1.70	2.44, 2.47	1.87
Hγ1/γ2	1.47	1.47	1.44	–	2.15
Hδ	3.05	3.03	3.07	–	–
Others	8.65, 7.41	8.85, 7.40	8.48, 7.40	–	–
$\Delta\delta/\Delta T$	−2.9	−2.3	−4.9	−4.9	−2.4

n.d. = not detected.

Table 2 summarizes all relevant chemical shifts together with temperature coefficients of the amide proton for all peptides examined. It can be observed that most chemical shifts are close to the values found for random conformations, whereas some temperature coefficients of amide protons are fairly small, e.g. -2.3 ppb/K for N^3, -2.4 ppb/K for Y^4 and -2.3 ppb/K for R^6 in peptide II. These data hint the presence of some structured conformers, but are not sufficient to indicate precise conformations nor, for that matter, to guarantee that the corresponding hydrogens are involved in intramolecular hydrogen bonds. However, NOE data support the hypothesis of a prevailing folded conformer in equilibrium with extended conformers.

A further general feature emerging from these experiments is that the eight peptides can be subdivided into two families, roughly parallelling the chemotactic behaviour. That is, the pattern of NOEs is similar for peptides I–IV and for peptides V–VIII, respectively. Accordingly, we decided to perform a detailed conformational analysis only on peptides II and VIII, considered as representative of the two families. In turn, this choice amounts to a comparison of the conformational properties of peptides carrying an acidic residue at the *N*-terminal position (and, consequently, a basic residue at the *C*-terminal position) *versus* peptides with the opposite distribution of charged residues.

NOESY spectra were acquired with mixing times ranging from 150 to 350 ms.

Figure 2 shows partial NOESY spectra of peptides II and VIII. Like peptide T itself, both peptides display many intraresidue and sequential NOEs in spite of the short chain length. However, the NOESY spectrum of peptide II contains also some medium

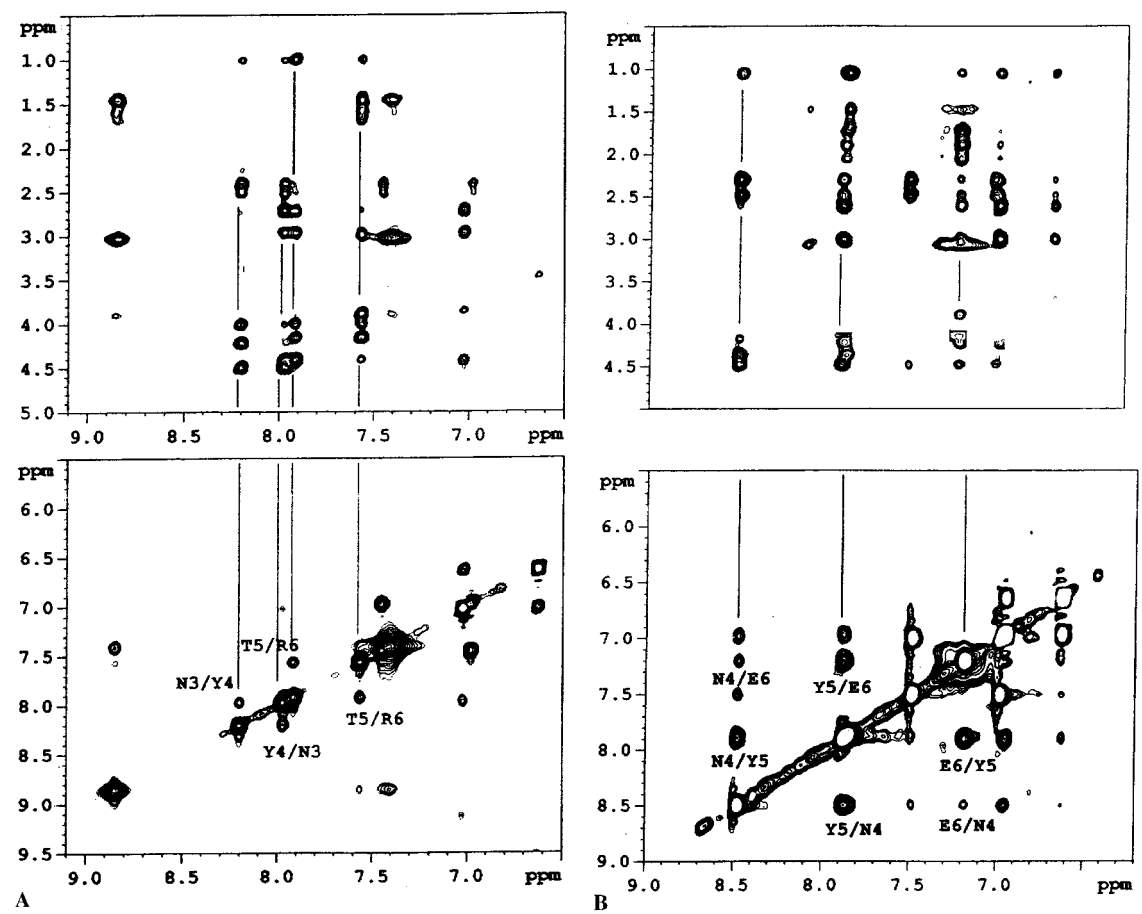

Figure 2 Partial NOESY spectra of peptides II (panel A) and VIII (panel B). The spectrum of peptide II was recorded at 400 MHz in neat DMSO-d_6 at 298 K with a mixing time of 200 ms. The spectrum of peptide VIII was recorded at 400 MHz in a DMSO-d_6 solution containing 10% v:v H_2O at 285 K using presaturation for water suppression and a mixing time of 300 ms.

range effects, such as those between the NH of Y^4 and αCH, βCH and γCH_3 of T^2, and also between the NH of T^6 and αCH and βCH_2 of Y^4. Although the coexistence of multiple conformational states cannot be ruled out based on these data, we did try to extract a prevailing folded conformer, on the assumption that all extended conformers in equilibrium with it should contribute only marginally to the pattern of NOEs. NOE cross-peaks were integrated with the program NMRView [14] and were translated into interproton distances with the routine CALIBA of DYANA [15]. This procedure afforded a total of 61 distance restraints (31 intraresidue and 30 sequential) for peptide II, and 62 distance restraints (28 intraresidue and 34 sequential) for peptide VIII. Introduction of these restraints in the standard annealing protocol of DYANA [15] generated 20 structures of each peptide with good values of the usual target function out of 40 random initial conformers. Satisfactory fits to the experimental NOEs were obtained: the few residual violations correspond mainly to NH_i-αCH_{i-1} effects, which presumably reflect a small contribution from extended conformers. The final ensemble of structures from DYANA has no violation greater than 0.79 Å in distance from the input restraints.

Figure 3 shows the bundles of structures of peptide II (panel A) and peptide VIII (panel B), obtained by superposition of the backbone atoms of residues 2–5.

In the case of peptide II, all structures in the bundle have similar values of dihedral angles but for terminal residues. The prevailing structure can be described as a 3_{10}-helix, although a subfamily of structures characterized by a single β-bend centered around residues *N-Y* is also present. In the case of peptide VIII, no prevailing canonical structure can be identified, probably because the number of diagnostic NOEs is not sufficient.

The 10 DYANA structures of peptide II with the lowest values of target function were subjected to energy minimization using the SANDER module of AMBER 5.0 [16], resulting in the bundle of structures shown in Figure 4. The molecular model of peptide II can be described as a quasi canonical 3_{10}-helix, as judged from deviations from idealized covalent geometry and from the two hydrogen bonds, the first between the NH of T^5 and the CO of T^2 and the second between the NH of R^6 and the CO of N^3. The same Figure shows for comparison the superposition of an idealized 3_{10}-helix.

Our conformational results are at variance with those of Cotelle *et al.* [27] who also describe peptide T as a 3_{10}-helix, but with a different localization with respect to the peptide sequence and with a different pattern of hydrogen bonds. However, it is in order to note that their peptide has all the side chains fully protected and *N*- and *C*-terminal groups protected by *tert*-butoxycarbonyl and benzyl groups, respectively. A fully protected peptide does not have, in general, the same biological properties of the parent, 'wild' peptide nor can easily assume the same conformation when protection of labile protons involves many of its residues.

DISCUSSION

The minimum sequence derived from peptide T that retains most of the biological activity, i.e. the *C*-terminal pentapeptide TTNYT, is probably representative of a widespread recognition motif.

We have investigated the occurrence, in protein data banks, of the two core sequences employed in

Figure 3 Stereoviews of the bundles of the ten structures with the lowest target function as obtained from the TAD (torsion angle dynamics) MD protocol of DYANA. The fit was obtained using the backbone atoms of residues 2–5 for both peptide II (panel A) and peptide VIII (panel B). R.m.s.d. values were 0.305 Å for peptide II and 0.268 Å for peptide VIII.

Figure 4 Stereo view of the bundle of the 10 best structures (superimposed using the backbone atoms of residues 2–5) of peptide II resulting from energy minimization with AMBER 5.0. A model of the same peptide with an idealized 3_{10}-helix geometry is superimposed as a neon representation.

the design of the hexapeptides studied in the present paper, namely, TNYT and TTNY. In order to generalize the search, we have allowed for the homology substitution of T with S, i.e. the patterns (written in the syntax of Swiss-Prot) we sought in the search were [TS]-*N*-*Y*-[TS] and [TS]-[TS]-*N*-*Y*. It is worth noting that both patterns are quite frequent in protein data banks, particularly in a large number of virus coat proteins, and may thus represent an important general feature of virus–host recognition. In a search performed in the Swiss-Prot Data Bank, the pattern [TS]-*N*-*Y*-[TS] was matched 866 times (127 of which from viruses) in 851 sequences (126 of which were viral proteins) out of 83857 entries and the pattern [TS]-[TS]-*N*-*Y* was matched 794 times (118 of which from viruses) in 776 sequences (111 of which were viral proteins) out of 83857 entries.

Furthermore, the amino acid sequence of peptide T shows homology with that of vasoactive intestinal peptide (VIP), a bioactive peptide which can also interact with the CD4 receptor [6], with sequence 39–46 of bovine lysozyme and with region 19–26 of the bovine pancreatic ribonuclease. The multiple alignment of these sequences, performed with the program CLUSTALX [28], is summarized in Figure 5. It is also interesting to recall that it has been recently reported that lysozymes from human milk and from chicken egg white [29] and both bovine pancreatic [29] and bovine seminal [30] ribonucleases possess activity against HIV-1. The similarity of biological activity may be based on conformational grounds. In order to substantiate this hypothesis it is useful to analyse the results of the structural study on our hexapeptides. As previously mentioned, the conformations of peptide T in DMSO solution suggested by qualitative NMR data [17] are a quasi-cyclic conformer characterized by a β-turn centred on the *N*-*Y* sequence of peptide T and a helical structure (either α or 3_{10}) involving the terminal pentapeptide [21]. In order to favour pseudo-cyclization, we put charged residues at both termini of the core sequence of peptide T. Reinforcement of the positive charge at the *N*-terminus with a basic residue and of the negative charge at the *C*-terminus with an acidic residue resulted indeed in pseudo-cyclic, albeit disordered structures (peptides V–VIII). This conformational preference, however, was parallelled by a decrease of chemotactic activity with respect to peptide T. On the other hand, the presence of residues carrying opposite charges, i.e. an acidic residue at the *N*-terminus and a basic residue at the *C*-terminus, favoured helical structures and was accompanied by retention of full chemotactic activity. This kind of conformational behaviour is not totally unexpected. Theoretical physical chemistry considerations, statistical analysis and experimental measurements on model peptides all point to a critical role played by charged groups in the stability of helical structures [31]. In particular, it has been observed that the presence of an acidic residue at the *N*-terminus stabilizes helical structures owing to a favourable interaction with the macroscopic electrostatic dipole of the helix [32]. It seems that in the case of

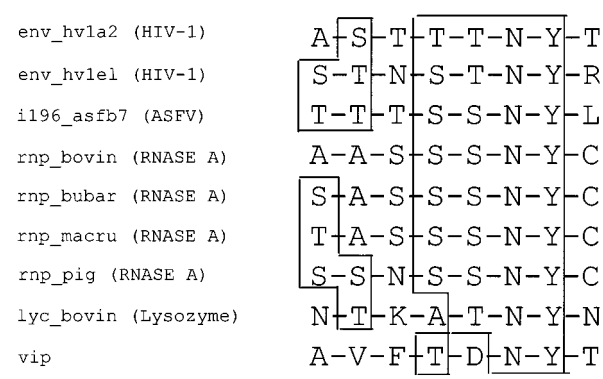

Figure 5 Alignment of the sequence of peptide T with those of bioactive peptides and selected sequences from exposed loops of proteins.

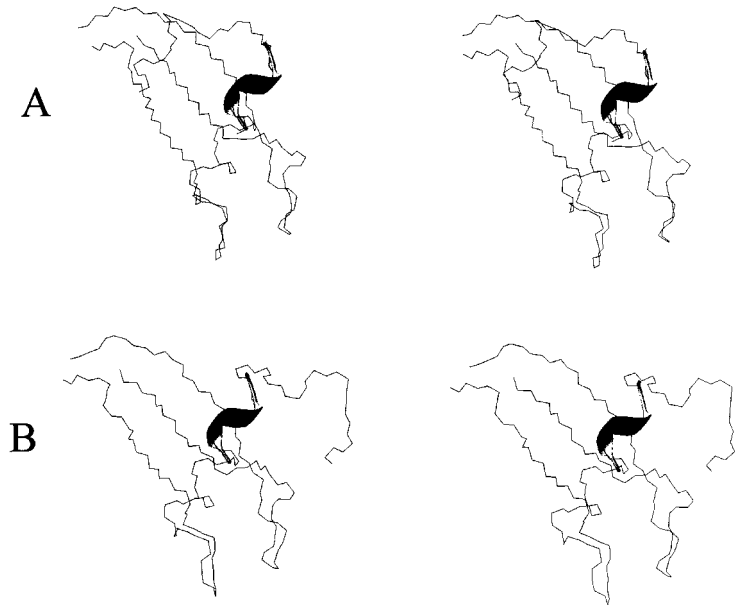

Figure 6 Overlap between the mean structure of the best 10 structures of peptide II and the X-ray structures of bovine pancreatic ribonuclease (7rsa.pdb, A) and bovine seminal ribonuclease (1bsr.pdb, B) around segment 23–26. The structures of bovine ribonucleases are shown as a line of backbone atoms, that of peptide II as a ribbon.

peptides II, this effect is prevailing with respect to the electrostatic interaction between the charged ends.

Accordingly, we can propose the helical structure of peptide II and its congeners, i.e. peptides I, III and IV, as plausible bioactive conformations.

Starting from these results and on the basis of the mentioned sequence homology, we compared the structural models of our peptides with the X-ray structure of both bovine pancreatic and bovine seminal ribonuclease. Figure 6 shows the overlap between the mean structure of peptide II and the X-ray structures of bovine pancreatic ribonuclease (7rsa.pdb, panel A) and bovine seminal ribonuclease (1bsr.pdb, panel B), obtained by superimposing the backbone atoms of the residues T^2–T^5 with the 23–26 region of the proteins. It can be observed that the structural model we propose for peptide II has a good superposition with the crystal structures of the proteins, with a r.m.s.d. of 0.617 Å and 0.624 Å, respectively. This result supports the hypothesis that the conformation of peptide II, selected on the basis of a chemotaxis assay, can indeed represent a structural model for the bioactive conformation adopted also for the anti-HIV activity.

Acknowledgements

This work was supported by grants from Regione Campania (Contributo POP 1994/1999 sottoprogramma 5, misura 5.4, azione 542), Italy.

REFERENCES

1. Pert CB, Hill JM, Ruff M, Berman RM, Robey WG, Arthur LO, Ruscetti FW, Farrar WL. Octapeptides deduced from the neuropeptide receptor-like pattern of antigen T4 in brain potently inhibit the human immunodeficiency virus receptor binding and T-cell infectivity. *Proc. Natl. Acad. Sci. USA* 1986; **83**: 9254–9258.
2. Baggiolini M. Chemokines and leukocyte traffic. *Nature* 1998; **392**: 565–568.
3. Cairns JS, D'Souza MP. Chemokines and HIV-1 second receptors: the theraupetic connection. *Nature Med.* 1998; **4**: 563–568.
4. Kwong PD, Wyatt R, Robinson J, Sweet RW, Sodroski J, Hendrickson WA. Structure of an HIV gp120 envelope glycoprotein in complex with the CD4 receptor and a neutralizing human antibody. *Nature* 1998; **393**: 648–659.
5. Brenneman DE, Buzy JM, Ruff MR, Pert CB. Peptide T sequences prevent neuronal cell death produced by

the envelope protein (gp120) of the human immunodeficiency virus. *Drug Develop. Res.* 1988; **15**: 361–369.
6. Ruff MR, Martin BM, Ginns EI, Farrar WL, Pert CB. CD4 receptor binding peptides that block HIV infectivity cause human monocyte chemotaxis. *FEBS Lett.* 1987; **211**: 17–22.
7. Marastoni M, Salvadori S, Balboni G, Scaranari V, Spisani S, Reali E, Traniello S, Tomatis R. Structure-activity relationships of cyclic and linear peptide T analogues. *Int. J. Pept. Protein Res.* 1993; **41**: 447–454.
8. Zigmond SH, Hirsch JG. Leukocyte locomotion and chemotaxis: new method for evaluation and demonstration of a cell derived chemotactic factor. *J. Exp. Med.* 1973; **137**: 387–395.
9. Bisaccia F, Castiglione-Morelli MA, Spisani S, Ostuni A, Serafini-Fracassini A, Bavoso A, Tamburro AM. The amino acid sequence coded by the rarely expressed exon 26A of human elastin contains a stable turn with chemotactic activity for monocytes. *Biochemistry* 1998; **37**: 11128–11135.
10. Piantini U, Soerensen OW, Ernst RR. Multiple quantum filters for elucidating NMR coupling networks. *J. Am. Chem. Soc.* 1982; **104**: 6800–6801.
11. Bax A, Davis DG. MLEV-17-based two-dimensional homonuclear magnetization transfer spectroscopy. *J. Magn. Reson.* 1985; **65**: 335–360.
12. Jeener J, Meyer BH, Bachman P, Ernst RR. Investigation of exchange processes by two dimensional NMR spectroscopy. *J. Chem. Phys.* 1979; **71**: 4546–4553.
13. Marion D, Wüthrich K. Application of phase sensitive two-dimensional correlated spectroscopy (COSY) for measurements of ^{1}H-^{1}H spin-spin coupling constants in proteins. *Biochem. Biophys. Res. Commun.* 1983; **113**: 967–971.
14. Johnson BA, Blevins RA. NMRView: a computer program for the visualization and analysis of NMR data. *J. Biomol. NMR* 1994; **4**: 603–614.
15. Güntert P, Mumenthaler C, Wüthrich K. Torsion angle dynamics for NMR structure calculation with the new program DYANA. *J. Mol. Biol.* 1997; **273**: 283–298.
16. Weiner SJ, Kollman PA, Nguyen DT, Case DA, Singh UC, Ghio C, Alagona G, Profeta S, Weiner PA. A new force field for molecular mechanical simulation of nucleic acids and proteins. *J. Am. Chem. Soc.* 1984; **106**: 765–784.
17. Picone D, Temussi PA, Marastoni M, Tomatis R, Motta A. A 500 MHz study of peptide T in a DMSO solution. *FEBS Letts.* 1988; **231**: 159–163.
18. Motta A, Picone D, Temussi PA, Marastoni M, Tomatis R. Conformational analysis of peptide T and its *C*-pentapeptide fragment. *Biopolymers* 1989; **28**: 479–486.
19. Shah D, Chen JM, Cart RP, Pincus MR, Scheraga HA. Correlation of α-bend conformations of tetrapeptides with their activities in CD4-receptor binding assays. *Int. J. Pept. Protein Res.* 1989; **34**: 235–241.
20. Filizola M, Centeno NB, Perez JJ. Computational study of the conformational domains of peptide T. *J. Pept. Sci.* 1997; **3**: 85–92.
21. Temussi PA, Picone D, Castiglione-Morelli MA, Motta A, Tancredi T. Bioactive conformation of linear peptides in solution: an elusive goal? *Biopolymers* 1989; **28**: 91–107.
22. Pert CB, Ruff MR. Peptide T (4–8): a pentapeptide sequence in the AIDS virus envelope which blocks infectivity is essentially conserved across nine isolates. *Clinical Neuropharm.* 1986; **9**: 482–487.
23. Rajan R, Awasthi SK, Bhattachajya S, Balaram P. Teflon-coated peptides: hexafluoroacetone trihydrate as a structure stabilizer for peptides. *Biopolymers* 1997; **42**: 125–128.
24. D'Ursi AM, Pegna M, Amodeo P, Molinari H, Verdini A, Zetta L, Temussi PA. Solution conformation of tuftsin. *Biochemistry* 1992; **31**: 9581–9586.
25. Sorimachi K, Craik DJ. Structure determination of extracellular fragments of amyloid proteins involved in Alzheimer's disease and Dutch-type hereditary cerebral haemorrhage with amyloidosis. *Eur. J. Biochem.* 1994; **219**: 237–251.
26. Amodeo P, Motta A, Picone D, Saviano G, Tancredi T, Temussi PA. Viscosity as a conformational sieve. NOE of linear peptides in cryoprotective mixtures. *J. Magn. Reson.* 1991; **95**: 201–207.
27. Cotelle N, Lohez M, Cotelle P, Henichart JP. Conformational study of the threonine-rich *C*-terminal pentapeptide of peptide T. *Biochem. Biophys. Res. Commun.* 1990; **171**: 596–602.
28. Higgins DG, Bleasby AJ, Fuchs R. CLUSTAL V: improved software for multiple sequence alignment. *CABIOS* 1991; **8**: 189–191.
29. Lee-Huang S, Huang PL, Sun Y, Huang PL, Kung HF, Blithe DL, Chen HC. Lysozyme and RNases as anti-HIV components in β-core preparations of human chorionic gonadotropin. *Proc. Natl. Acad. Sci. USA* 1999; **96**: 2678–2681.
30. Youle RJ, Wu YN, Mikulski SM, Shogen K, Hamilton RS, Newton D, D'Alessio G, Gravell M. RNase inhibition of human immunodeficiency virus infection of H9 cells. *Proc. Natl. Acad. Sci. USA* 1994; **91**: 6012–6016.
31. Shoemaker KR, Kim PS, York EJ, Stewart JM, Baldwin RL. Tests of the helix dipole model for stabilization of α-helices. *Nature* 1987; **326**: 563–567.
32. Serrano L, Fersht AR. Capping and α-helix stability. *Nature* 1989; **342**: 296–299.

